2026 RISP International Workshop on Nonlinear Circuits, Communications and Signal Processing
February 27 - March 2, 2026, Honolulu, Hawaii, U.S.A.

Performance of Chaotic Time Series Prediction Using a Spiking Reservoir with an Excitation Layer and an Inhibition Layer

Tomoki Goto, Yoko Uwate and Yoshifumi Nishio

Department of Electrical and Electronic Engineering, Tokushima University
2-1 Minami-Josanjima, Tokushima 770-8506, Japan
E-mail: {tomoki, uwate, nishio}@ee.tokushima-u.ac.jp

Abstract

In this study, a structural design is investigated to improve the stability of autonomous prediction of chaotic time series using a spiking neural network (SNN) as a reservoir. A two-layer SNN reservoir composed of excitatory and inhibitory (E/I) neurons is constructed, and the prediction output is learned by updating only the readout weights online using FORCE (RLS). Using the Lorenz system as a benchmark, NRMSE is evaluated by separating the training (teacher-forcing) and closed-loop autonomous segments; the results indicate that the two-layer architecture reproduces key waveform features and that the autonomous-segment prediction accuracy varies with the E/I ratio.

1. Introduction

Chaotic time series exhibit high sensitivity to initial conditions: even small errors can rapidly amplify over time, making reliable long-horizon prediction difficult [1]. Nevertheless, chaotic behavior appears in a wide range of real-world phenomena, including meteorology, fluid dynamics, biological signals, and mechanical vibrations [2]. Accurate prediction of such dynamics is important for control-system modeling, anomaly detection, and sensor-signal analysis. In practical deployments, online processing and edge-side inference are often required, which motivates prediction methods that deliver high accuracy under constraints on computation and power.

Reservoir computing (RC) provides a computationally efficient framework in which recurrent connections are fixed and only the readout weights are learned, enabling fast training and simple implementation for time-series processing. A representative RC model, the Echo State Network (ESN), approximates nonlinear dynamics by learning a linear readout while keeping the internal recurrent weights fixed. More recently, spiking neural networks (SNNs) have been explored as reservoirs because spike-based representations are well suited to low-power neuromorphic hardware and naturally capture temporal structure in sensor time series. However, the dynamics of SNN reservoirs can become overly amplified or excessively damped depending on connection strength and the excitatory/inhibitory (E/I) balance [3]. As a result, even when accurate tracking is achieved during the teacher-forced learning phase, closed-loop autonomous prediction with output feedback can become unstable.

Motivated by stability mechanisms observed in biological neural circuits, excitatory/inhibitory (E/I) structure has been regarded as a key factor for regulating network activity. In particular, balanced excitation and inhibition is believed to suppress runaway activity while maintaining rich, expressive dynamics. However, the extent to which the E/I ratio and connectivity in SNN reservoirs affect autonomous closed-loop prediction performance for chaotic time series has not yet been systematically characterized. Moreover, parallel reservoir configurations can be constructed by partitioning the reservoir into multiple sub-reservoirs [4]. Such configurations may diversify internal representations and potentially improve stability, but effective design conditions for spiking reservoirs remain unclear.

In this study, an SNN reservoir is constructed with Dale's principle enforced by constraining each neuron's outgoing synapses to have a fixed sign (excitatory or inhibitory). FORCE learning based on recursive least squares (RLS) is adopted to update only the readout weights online [5]. Chaotic waveforms generated by the Lorenz system are used as prediction targets, and performance is evaluated using the normalized root-mean-square error (NRMSE) by separating a warm-up and teacher-forcing segment from a closed-loop autonomous segment in which the predicted output is fed back as the input. Parameter sweeps of the E/I ratio are conducted to identify structural conditions that improve autonomous prediction stability. The results indicate that autonomous-segment performance depends strongly on the E/I balance and that an appropriate E/I ratio yields lower autonomous NRMSE and reduced trial-to-trial variability, while excessively excitation- or inhibition-dominant settings degrade stability. These observations provide practical guidance for selecting E/I ratios when designing spiking reservoirs for stable closed-loop prediction.

2. Proposed Model

2.1 Spiking Neuron Model

This study employs spiking neurons that represent and propagate information as spike trains (discrete events), unlike conventional analog neuron models that directly handle continuous-value signals. Spikes from presynaptic neurons form postsynaptic currents via synapses, and the membrane potential is updated as the time integral of these currents. An output spike is generated when the membrane potential exceeds a threshold, and the membrane potential is reset. Figure 1 shows the processing flow from input spike to output spike generation.

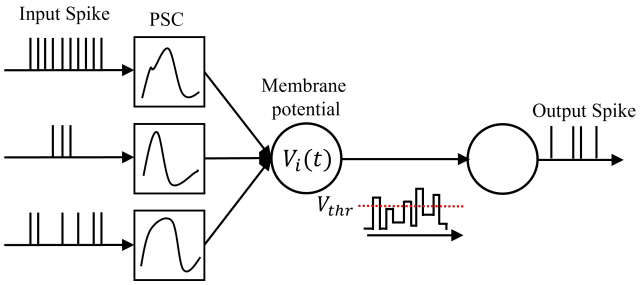

Figure 1: Spike transmission and spike generation.

The spiking neuron model employs the Leaky Integrate-and-Fire (LIF) model. The LIF model concisely describes the integration of membrane potential in response to input current, decay due to leakage, and firing upon threshold crossing. Let the membrane potential of neuron i be $V_i(t)$, the resting membrane potential be V_{rest}, the membrane time constant be τ_m, and the input current be $I_i(t)$. The time evolution of the membrane potential is expressed by the following equation:

$$\tau_m \frac{dV_i(t)}{dt} = -(V_i(t) - V_{\mathrm{rest}}) + I_i(t). \tag{1}$$

With a simulation time step Δt, the membrane potential dynamics is discretized using the forward Euler method as follows:

$$V_i[t+1] = V_i[t] + \frac{\Delta t}{\tau_m}\left(V_{\mathrm{rest}} - V_i[t] + I_i[t]\right). \tag{2}$$

A spike is generated when the updated membrane potential exceeds a threshold V_{thr}:

$$V_i[t+1] \geq V_{\mathrm{thr}} \Rightarrow s_i[t+1] = 1, \tag{3}$$

and otherwise $s_i[t+1] = 0$. After firing, the membrane potential is reset to V_{reset}:

$$V_i[t+1] \leftarrow V_{\mathrm{reset}}. \tag{4}$$

Here $s_i[t] \in \{0, 1\}$ denotes the discrete spike train, which provides the nonlinearity essential for reservoir computing.

2.2 Double-exponential synapse model

Presynaptic spikes are converted into a postsynaptic current (PSC) through synaptic filtering and subsequently injected into the neuron dynamics. A double-exponential synapse is employed with rise and decay time constants τ_r and τ_d respectively. To match the implementation, an auxiliary synaptic state $x_i[t]$ and the PSC state $y_i[t]$ are introduced, which are updated as follows:

$$y_i[t+1] = \left(1 - \frac{\Delta t}{\tau_r}\right) y_i[t] + \Delta t x_i[t], \tag{5}$$

$$x_i[t+1] = \left(1 - \frac{\Delta t}{\tau_d}\right) x_i[t] + \frac{J_i[t]}{\tau_r \tau_d}. \tag{6}$$

The recurrent drive $J_i[t]$ is defined in the next subsection. The PSC $y_i[t]$ is added to the total input current $I_i[t]$.

2.3 Recurrent connectivity and E/I definition

Let $\Omega \in \mathbb{R}^{N \times N}$ be the recurrent weight matrix of a reservoir with N neurons. Given spike trains $s_i[t]$, the instantaneous recurrent drive is defined as

$$J_j[t] = \sum_{i=1}^{N} \Omega_{ji} s_i[t]. \tag{7}$$

In the implementation, columns correspond to presynaptic neurons (presynaptic indexing), and $J[t]$ is computed by summing the columns associated with the presynaptic neurons that spike at time t.

Excitatory and inhibitory neurons are defined by imposing a Dale-type sign constraint on the outgoing connections of each presynaptic neuron:

$$i \in \mathcal{E} \Rightarrow \Omega_{ji} \geq 0, \qquad i \in \mathcal{I} \Rightarrow \Omega_{ji} \leq 0. \tag{8}$$

2.4 Readout and FORCE learning for the proposed architecture

Following the reservoir computing paradigm, the recurrent weights Ω are fixed and only the readout weights are trained. Let $r[t]$ be the filtered spike-based state used for decoding (obtained by synaptic filtering of spikes). The output is given by a linear readout

$$z[t] = \Phi^{\top} r[t]. \tag{9}$$

The readout weights Φ are updated online using FORCE learning (RLS) during the training window $[t_{\min}, t_{\mathrm{crit}})$. Performance is evaluated separately in the training (teacher-forcing) segment and the autonomous (closed-loop) segment. In the autonomous segment, prediction is continued by feeding back the model output as the input.

A two-reservoir parallel architecture without inter-layer coupling is also considered. Figure 2 illustrates the overall

architecture: two independent spiking reservoirs generate filtered states$r_1[t]$ and $r_2[t]$, which are linearly combined by trainable readouts and summed to produce the output $z[t]$.

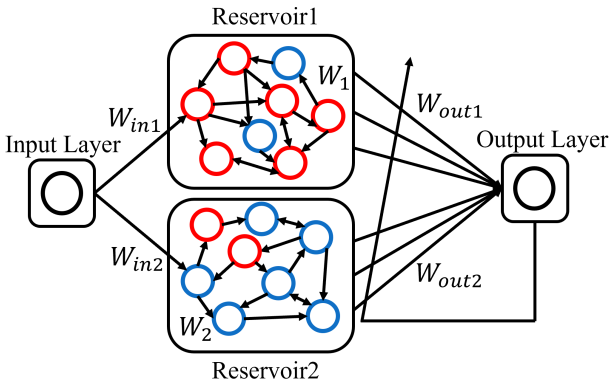

Figure 2: Two-reservoir parallel architecture without inter-layer coupling.

Each reservoir transforms the input into a high-dimensional spiking state, and the final prediction is obtained by summing two linear readouts trained by FORCE (RLS). The outputs from two independent reservoirs are combined as

$$z[t] = \Phi_1^\top r_1[t] + \Phi_2^\top r_2[t]. \tag{10}$$

By varying the E/I ratio of each reservoir, structural conditions that improve autonomous prediction stability are investigated.

3. Results

The proposed spiking reservoir computing model is evaluated on the Lorenz system using the normalized x-component. The simulation is divided into three segments: a warm-up period, a teacher-forcing training period $[t_{\min}, t_{\text{crit}})$ in which the readout is updated by FORCE (RLS), and an autonomous (closed-loop) period $[t_{\text{crit}}, T)$. Performance is quantified by NRMSE computed separately in the full, teacher-forcing, and autonomous segments.

3.1 Prediction waveforms in teacher-forcing and autonomous segments

Figure 3 shows representative target and predicted signals. The figure provides a zoomed view around the transition time and visualizes the prediction in two segments (40 to 45 s and 45 to 50 s), separated by the vertical dashed line at $t_{crit} = 45$ s. During the teacher-forcing segment, the trained readout tracks the target waveform, indicating that the fixed spiking reservoir provides a suitable nonlinear temporal basis for decoding. In particular, the prediction output in 40 to 45 s (green) closely overlaps the target, demonstrating successful tracking under teacher forcing. In the autonomous segment, the model continues prediction in closed loop; stability depends on the reservoir configuration, especially the E/I balance and the reservoir architecture. After switching to the autonomous segment (45 to 50 s, orange), the output is generated in closed loop and deviations from the target can be observed, which motivates the stability analysis in the subsequent experiments.

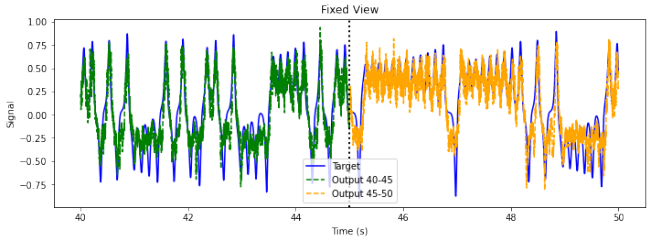

Figure 3: Zoomed prediction results around the transition from teacher forcing to autonomous prediction, where $t_{crit} = 45$ s separates the teacher-forcing segment (40 to 45 s, green) and the closed-loop autonomous segment (45 to 50 s, orange).

3.2 Autonomous NRMSE under Different E/I Ratios

A parameter sweep of the E/I ratio is conducted for the two-reservoir model,and the autonomous-segment NRMSE is evaluated. Figure 4 summarizes the NRMSE statistics (maximum, minimum, and average) across trials for each E/I ratio. The results indicate that the prediction performance depends on the E/I balance, and more excitation-dominant settings tend to yield lower average NRMSE in the tested range. The gap between the maximum and minimum NRMSE also decreases as the E/I ratio becomes more excitation-dominant, suggesting improved robustness to trial-to-trial variability.

3.3 Firing-rate distributions in excitatory and inhibitory populations

To verify that the observed prediction performance is not achieved in degenerate spiking regimes, firing-rate distributions are analyzed separately for the excitatory and inhibitory populations. Figure 5 shows firing-rate histograms for the full sequence (blue), the teacher-forcing segment $[t_{\min}, t_{\text{crit}})$ (orange), and the autonomous segment $[t_{\text{crit}}, T)$ (green). The upper panel corresponds to the excitatory population, whereas the lower panel corresponds to the inhibitory population.The excitatory population exhibits sustained activity across segments and becomes more active in the autonomous segment, as indicated by a rightward shift of the firing-rate distribution in the upper panel (green) relative to the teacher-

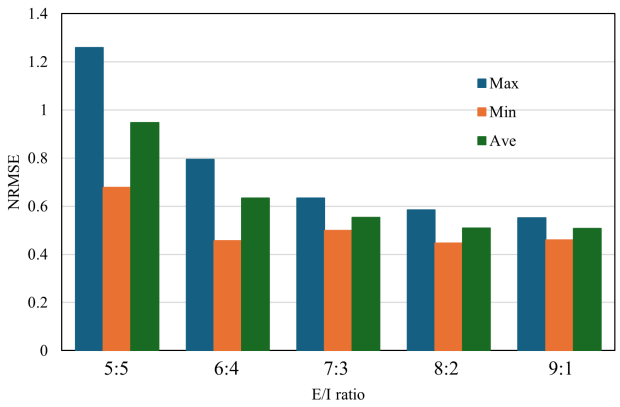

Figure 4: Autonomous-segment NRMSE statistics (max/min/average across trials) for different E/I ratios in the two-reservoir model.

forcing segment (orange). Despite this increase, the distribution remains bounded and does not collapse to silence or concentrate at extremely high rates. In contrast, the inhibitory population shows a larger fraction of low-rate neurons, yet retains nonzero activity in all segments. These results support that the network operates in a non-degenerate dynamical regime and that the autonomous prediction behavior is evaluated under stable spiking activity rather than trivial silence or saturation.

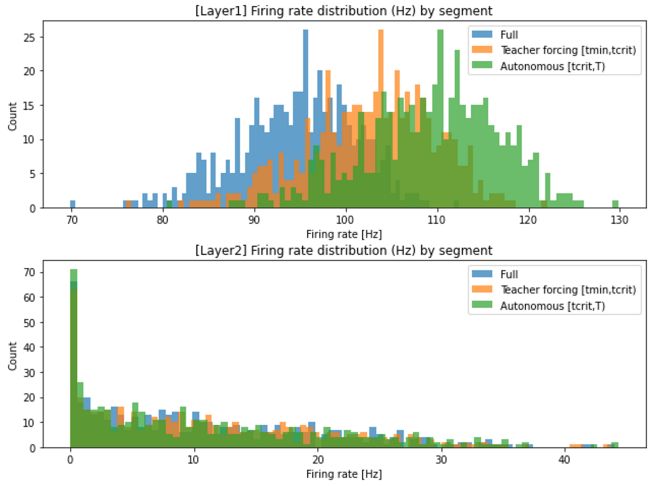

Figure 5: Firing-rate histograms of excitatory (top) and inhibitory (bottom) populations for the full sequence (blue), teacher-forcing segment $[t_{\min}, t_{\mathrm{crit}})$ (orange), and autonomous segment $[t_{\mathrm{crit}}, T)$ (green).

4. Conclusion

This study investigated spiking reservoir computing for chaotic time-series prediction using an LIF network with double-exponential synapses and FORCE (RLS) readout learning. A presynaptic (column-wise) Dale-type sign constraint was imposed to define excitatory and inhibitory neurons, and the spectral radius was normalized to control the dynamical scale while keeping the reservoir connections fixed.

Experiments on the Lorenz system showed that autonomous (closed-loop) prediction stability depends on the E/I balance and that a suitable E/I ratio yields more stable autonomous performance than strongly excitation-dominant or inhibition-dominant settings. Firing-rate distributions indicate that the observed performance is achieved without activity collapse or saturation. Future work will quantify the underlying mechanisms via time-scale and memory-related metrics and extend the approach toward efficient neuromorphic implementations.

Acknowledgment

This work was partly supported by JSPS KAKENHI Grant Number JP25K15273.

References

[1] Abarbanel, H. D. I., Brown, R., Sidorowich, J. J., and Tsimring, L. S. ”The analysis of observed chaotic data in physical systems,” *Rev. Mod. Phys.*, 65(4), 1331-1392, 1993.

[2] Zhuang, Y., Almeida, M., Ding, W., Islam, S. M. Atiqul, Li, Z., and Chen, P. ”Horizon Forcing: Improving the Recurrent Forecasting of Chaotic Systems,” *ACM Trans. Intell. Syst. Technol.*, 16(5), Article 120 (pp. 120:1-120:22), 2025.

[3] George, A. M., Dey, S., Banerjee, D., Mukherjee, A., and Suri, M. ”Online time-series forecasting using spiking reservoir,” *Neurocomputing*, 518, 82-94, 2023.

[4] Srinivasan, K., Plenz, D., and Girvan, M. ”Boosting reservoir computing with brain-inspired adaptive control of E-I balance,” *Nat. Commun.*, 16, 10212, 2025.

[5] Nicola, W.,and Clopath, C. ”Supervised learning in spiking neural networks with FORCE training,” *Nat. Commun*, 8(1), 2208, 2017.